forests

MDPI

Article

Metabarcoding of Bacteria Associated with the Acute Oak Decline Syndrome in England

Melanie Sapp [1,*], Erin Lewis [1], Stephen Moss [2], Ben Barrett [1], Susan Kirk [3], John G. Elphinstone [1] and Sandra Denman [3]

1 Fera, Sand Hutton, York YO41 1LZ, UK; erin.lewis@fera.co.uk (E.L.); ben.barrett@fera.co.uk (B.B.); john.elphinstone@fera.co.uk (J.E.)
2 Department of Biology, University of York, Heslington, York YO10 5DD, UK; stephen.moss@york.ac.uk
3 Forest Research, Alice Holt Lodge, Farnham, Surrey GU10 4LH, UK; susan.kirk@forestry.gsi.gov.uk (S.K.); sandra.denman@forestry.gsi.gov.uk (S.D.)
* Correspondence: melanie.sapp@hhu.de; Tel.: +49-211-8113656; Fax: +49-211-8112817

Academic Editors: Jan Stenlid, Jonas Oliva and Audrius Menkis
Received: 30 October 2015; Accepted: 19 April 2016; Published: 26 April 2016

Abstract: Outbreaks of acute oak decline (AOD) have been documented in England from 2006. Both species of native oaks (*Quercus robur* and *Quercus petraea*) are affected. To complement isolation efforts for identification of putative causative biotic agents and increase our understanding of bacteria associated with oak tissue, five sites in England were chosen for this study. Samples of outer bark, inner bark, sapwood and heartwood were taken from healthy oak and trees with symptoms at varying stages of the syndrome. Furthermore, larval galleries attributed to infestation with *Agrilus biguttatus* were included. After DNA extraction and amplification of the V3–V5 fragment of the bacterial 16S rRNA genes by pyrosequencing, the dataset was analyzed to identify patterns in bacterial communities in oak tissue samples with and without AOD symptoms at each site. The composition of bacterial communities differed greatly according to the site from which the samples were obtained. Within each site, the composition of the bacteria associated with symptomatic tissue varied between advanced stages of the syndrome and healthy tissue. Key players in healthy and symptomatic tissue were identified and included members of the Gammaproteobacteria related to *Pseudomonas* sp. or *Brenneria goodwinii* and members of the Firmicutes.

Keywords: oak associated microbiome; pyrosequencing; 16S rRNA gene; acute oak decline; endosphere; native oak

1. Introduction

Acute oak decline (AOD) appears to be a complex, secondary disease of native oak (*Quercus robur* and *Q. petraea*), and is increasingly found on turkey oak (*Q. cerris*) in the UK. It is widespread across England and the Welsh borders, with northerly limits in the counties of Cheshire, Derbyshire, Lincolnshire and Nottinghamshire (around the 53° N latitude) and westerly limit along the Welsh borders [1,2]. Quantitative studies on the number of trees affected have not been carried out, but estimates from the sector suggest many thousands of oak trees are affected.

The decline is characterised by two distinctive symptoms (stem bleeds and internal bark decay) and two signs (exit holes on tree stems and larval galleries in the inner bark tissues). It is considered a distinctive condition within the wider oak decline complex [1]. To date research indicates a complex cause of the lesions and bark decay in the inner bark tissues. Using destructive sampling and isolation studies an insect and bacterial component were revealed [3]. As a large number of microbes are not tractable to culture, additional methods are required to identify as many putative necrogenic organisms

as possible. Here, we present data derived from a metabarcoding technique to gain insights into the community structure of affected and healthy oak trees from five sites in England.

Advances in high throughput sequencing are helping to unravel the composition and identity of the vast diversity of microorganisms in various habitats. Such habitats include eukaryotic hosts for whose microbiomes strong differentiation into microniches can be shown [4–7].

It is generally thought that the plant microbiome serves several functions for its host ranging from growth stimulation and providing a competitive advantage for resource acquisition to other mechanisms such as suppressing damaging microbes, and enhancing stress resistance, and nutrient transport ([8] and references therein). The composition of the microbiomes of phyllospheres and rhizospheres have been widely studied for several plant species [9]. In general, a particularly large bacterial diversity has been observed in the rhizosphere of a wide range of plants with 10^4 bacterial species detected [10–12]. Interestingly, rhizosphere associated microorganisms were shown to influence the plant's immune response and inversely, plants were capable of influencing their rhizosphere microbiome ([10] and references therein) implicating elaborate relationships. Studies analyzing factors shaping the phyllosphere microbiome were carried out in various scales, ranging from the landscape level (covering a range of different plant species) to the individual level (where the different plant parts of various genotypes of a single species were investigated). There is consensus that the phyllosphere microbiome is less taxa rich than the rhizosphere microbiome. The microbiome can vary between different plant species, for example trees. There were less than 100 taxa associated with Ginkgo trees [13]; but several hundred bacterial species detected on a number of tree species including *Metrosiderospolymorpha* [6], Tamarix trees [14], and various trees sampled in forests of Brazil [15] and Panama [16]. Strong differences in the phyllosphere were attributed to plants' functional traits [16], although variation was observed in relation to season and shorter timescales ([17] and references therein). These findings imply that the phyllosphere responds to species specific characteristics as well as plant genotype [18,19]. Furthermore, physiological changes of the hosts as well as environmental factors, including the distance of the organ to soil [7], can influence the phyllosphere community structure ([17] and references therein). Spatial structuring at the plant part level [6,7,13] suggests the adaptation of specific taxa to available microniches within a plant's phyllosphere, whereas on a larger scale, geographical distance [14] shapes phyllosphere communities as shown for Tamarix trees.

Many studies have focused on the ectosphere (outer surfaces, [8]), studying the epi- and endophytic microbiome of plant organs as in the case of the phyllosphere [8], partly due to its accessibility for sampling. The current study focused on the oak's stem endosphere and its associated microbiome. In general, endophytic microbes residing within plant tissues (the endosphere), whether in leaves, roots or stems, can establish beneficial, neutral or detrimental associations of varying intimacy with their host plants. Since woody tissue is such a specific niche, adaptation of microorganisms to the compounds present is required for growth and survival. For example the type and composition of carbohydrates [20], phenolic compounds [21], and other extractables [22] in woody stems can vary. Furthermore, studies have shown differences even between different trees in dry extract (dry wood), ellagitanins and ellagic acid, as well as whisky-lactone extracted from pedunculate and sessile oaks in France [22]. Variation was also discovered in the aromatic compounds present in woody stems [23,24], for which geographical origin can be partly a determining factor ([21] and references therein) as it varies in environmental factors like soil type, sun exposure and rainfall [21].

Despite the specific niche woody tissue provides, some organisms are adapted to utilize this environment as a food source. It can therefore be the place of microbial attack [25–29]. Primary plant pathogens are usually studied using classic microbiology, including isolation of microbes from an environment on nutrient media to obtain cultures of the pathogens involved, which often misses important microbial diversity. New technologies like metabarcoding can complement traditional investigative methods and since the plant microbiome is a key determinant of plant health and productivity [10], it has received substantial attention in recent years [9,30]. Previous studies focusing on identifying unknown bacterial taxa from oak trees suffering from AOD have used classical

microbiology. Various gram-negative bacteria of the family Enterobacteriaceae have been associated with AOD symptoms including *Gibbsiella quercinecans* [31], *Lonsdalea quercina* ssp. *britannica* [32], *Brenneria goodwinii* [33], *Gibbsiella greigii* [34], a range of species of the genus *Rahnella* [35], and *Brenneria roseae* ssp. *roseae* [36]. This metabarcoding study aimed to supplement those efforts and helps to further understand the plant:microbial interactions taking place within oak trees affected or not affected by the AOD syndrome. Specifically, high-throughput sequencing technologies were used to identify thousands of sequences per sample and thus attempt to reveal the various taxa and their relative abundance interacting in healthy and diseased trees, including any rare or uncultivable microbial species. Thus, the 16S rRNA gene, the most comprehensive taxonomic marker available to date [37,38] was selected for metabarcoding.

To our knowledge this is the first study of the bacterial microbiome associated with oak bark and internal tissue. We hypothesized that we would find spatial structuring of the microbial community at different levels from landscape scale to within tree tissue types. Furthermore, we expected that the microbiomes would differ according to the health status of trees.

2. Experimental Section

2.1. Sampling

Five sites, representative of the known distribution of AOD in England, were selected for this study based on the availability of representative material and the willingness of the landowners to donate and fell affected trees for research. The sites chosen were: Attingham Wood (AW, OS Eastings 356033, OS Northings 310372), Bisham Wood (BW, OS Eastings 485362, OS Northings 184100), Great Monks Wood (GMW, OS Eastings 582100, OS Northings 225300); Stratfield Brake (SB, OS Eastings 449400, OS Northings 211900) and Runs Wood (RW, OS Eastings 563207, OS Northings 310858) (Table 1). At BW and SB only two trees at each site were sampled, a healthy and a diseased tree with advanced symptoms. At GMW, an early stage symptomatic tree was included bringing the number of trees sampled there to three; and at the two remaining sites, AW and RW, an additional category of tree was included, those showing moderate symptoms, bringing the total to four trees sampled on both these sites. Trees were sampled as described by Denman *et al.* [1] and summarized below. The location of each tree was recorded using GPS (Garmin GPSmap 60CSx—Global Positioning Systems, UK) for mapping and recording purposes. Diameter at breast height (DBH, *i.e.*, 1.3 m) was measured using a Forestry Suppliers metric diameter tape to get an indication of age/maturity of the tree. Severity of AOD attack was assessed by categorizing the number of bleeding points on stems where more than 20 stem bleeds per tree trunk scored advanced/severe; between 10 and 20 bleeds was moderate and less than 10 bleeds was considered a light (early) infection; healthy trees showed no stem bleeds at all. A sharp, surface disinfected chisel was used to remove a fully barked panel taken to a 5–7 cm depth in the heartwood. Panels were approximately 20 cm × 15 cm (LxB). The sampling equipment was thoroughly surface disinfected by dousing with industrial methylated spirits for 2 min and wiping dry with sterile paper towels, between samples. Each symptomatic panel was selected to include one or more bleed points, and both bark and wood tissues. On each of the symptomatic trees a non-symptomatic panel was cut some distance from the panel with symptoms. Healthy tree panels and non-symptomatic panels in a symptomatic tree did not have stems bleeds. Once cut, it was placed in a clean polythene bag, kept cool and taken to the laboratory for processing. Material to be processed was kept in a cold room at 4 °C overnight and was sorted, packaged and posted within 24 h of the field sampling. During the sorting process each panel was manually separated into outer bark, inner bark, sapwood and heartwood tissues by clamping the panel in a vice grip and prising the tissues apart using a disinfected chisel. Where galleries were present (*i.e.*, in symptomatic tissues only), small blocks of tissue were chiseled out containing the galleries. Blocks of material were placed in clean plastic zip-lock bags, placed in a cooler with ice blocks and shipped overnight to the laboratory where they were processed as described below.

Table 1. Bacteria 16S rRNA gene sequences after denoising of pyrosequencing data.

Sample	Sequences after Denoising	Symptom Status of Tree	Symptom Status of Tissue	Tissue	Site	Barcode Sequence
GMW2	3293	Healthy	Healthy	Inner bark	GMW	ACGAGTGCGT
GMW3	3586	Healthy	Healthy	Sapwood	GMW	ACGCTCGACA
GMW6	4255	AOD	Symptomatic	Inner bark	GMW	AGACGCACTC
GMW7	3138	AOD	Symptomatic	Sapwood	GMW	AGCACTGTAG
GMW9	3498	AOD	Symptomatic	Gallery	GMW	ATCAGACACG
GMW11	3509	AOD	Non-symptomatic	Inner bark	GMW	ATATCGCGAG
GMW12	3829	AOD	Non-symptomatic	Sapwood	GMW	CGTGTCTCTA
GMW6 *	3893	AOD	Symptomatic	Inner bark	GMW	CTCGCGTGTC
GMW7 *	3798	AOD	Symptomatic	Sapwood	GMW	TAGTATCAGC
GMW9 *	3847	AOD	Symptomatic	Gallery	GMW	TCTCTATGCG
GMW11 *	3975	AOD	Non-symptomatic	Inner bark	GMW	TGATACGTCT
GMW12 *	3689	AOD	Non-symptomatic	Sapwood	GMW	TACTGAGCTA
R1	1138	Healthy	Healthy	Outer bark	RW	ACGAGTGCGT
R2	1061	Healthy	Healthy	Inner bark	RW	ACGCTCGACA
R3	826	Healthy	Healthy	Sapwood	RW	AGACGCACTC
R4	1019	Healthy	Healthy	Heartwood	RW	AGCACTGTAG
R5	633	AOD	Symptomatic	Outer bark	RW	ATCAGACACG
R6	727	AOD	Symptomatic	Inner bark	RW	ATATCGCGAG
R7	887	AOD	Symptomatic	Sapwood	RW	CGTGTCTCTA
R8	968	AOD	Symptomatic	Heartwood	RW	CTCGCGTGTC
R9	910	AOD	Symptomatic	Gallery	RW	TAGTATCAGC
R10	980	AOD	Non-symptomatic	Outer bark	RW	TCTCTATGCG
R11	7569	AOD	Non-symptomatic	Inner bark	RW	TGATACGTCT

Table 1. *Cont.*

Sample	Sequences after Denoising	Symptom Status of Tree	Symptom Status of Tissue	Tissue	Site	Barcode Sequence
R12	8490	AOD	Non-symptomatic	Sapwood	RW	TACTGAGCTA
R13	8088	AOD	Non-symptomatic	Heartwood	RW	ACGAGTGCGT
R14	7795	AOD	Symptomatic	Outer bark	RW	ACGCTCGACA
R15	7440	AOD	Symptomatic	Inner bark	RW	AGACGCACTC
R16	7969	AOD	Symptomatic	Sapwood	RW	AGCACTGTAG
R17	4444	AOD	Symptomatic	Heartwood	RW	ATCAGACACG
R18	10658	AOD	Symptomatic	Gallery	RW	ATATCGCGAG
R19	7535	AOD	Non-symptomatic	Outer bark	RW	CGTGTCTCTA
R20	6931	AOD	Non-symptomatic	Inner bark	RW	CTCGCGTGTC
R21	7303	AOD	Non-symptomatic	Sapwood	RW	TAGTATCAGC
R22	6873	AOD	Non-symptomatic	Heartwood	RW	TCTCTATGCG
R23 *	5395	AOD	Symptomatic	Outer bark	RW	TGATACGTCT
R24 *	9518	AOD	Symptomatic	Inner bark	RW	TACTGAGCTA
R25 *	8223	AOD	Symptomatic	Sapwood	RW	ACGAGTGCGT
R26 *	6742	AOD	Symptomatic	Heartwood	RW	ACGCTCGACA
R27 *	10902	AOD	Symptomatic	Gallery	RW	AGACGCACTC
R28 *	7134	AOD	Non-symptomatic	Outer bark	RW	AGCACTGTAG
R29 *	4855	AOD	Non-symptomatic	Inner bark	RW	ATCAGACACG
R30 *	7838	AOD	Non-symptomatic	Sapwood	RW	ATATCGCGAG
R31 *	7314	AOD	Non-symptomatic	Heartwood	RW	CGTGTCTCTA
A1	4168	Healthy	Healthy	Outer bark	AW	CTCGCGTGTC
A2	3320	Healthy	Healthy	Inner bark	AW	TAGTATCAGC
A3	4221	Healthy	Healthy	Sapwood	AW	TCTCTATGCG
A4	3228	Healthy	Healthy	Heartwood	AW	TGATACGTCT
A5	4448	AOD	Symptomatic	Outer bark	AW	TACTGAGCTA
A6	10358	AOD	Symptomatic	Inner bark	AW	ACGAGTGCGT
A7	3664	AOD	Symptomatic	Sapwood	AW	ACGCTCGACA

Table 1. *Cont.*

Sample	Sequences after Denoising	Symptom Status of Tree	Symptom Status of Tissue	Tissue	Site	Barcode Sequence
A8	2067	AOD	Symptomatic	Heartwood	AW	AGACGCACTC
A9	2528	AOD	Symptomatic	Gallery	AW	AGCACTGTAG
A10	3556	AOD	Non-symptomatic	Outer bark	AW	ATCAGACACG
A11	9465	AOD	Non-symptomatic	Inner bark	AW	ATATCGCGAG
A12	3186	AOD	Non-symptomatic	Sapwood	AW	CGTGTCTCTA
A13	2698	AOD	Non-symptomatic	Heartwood	AW	CTCGCGTGTC
A14	5970	AOD	Symptomatic	Outer bark	AW	TAGTATCAGC
A15	4036	AOD	Symptomatic	Inner bark	AW	TCTCTATGCG
A16	3969	AOD	Symptomatic	Sapwood	AW	TGATACGTCT
A17	9214	AOD	Symptomatic	Heartwood	AW	TACTGAGCTA
A18	5015	AOD	Symptomatic	Gallery	AW	ACGAGTGCGT
A19	4404	AOD	Non-symptomatic	Outer bark	AW	ACGCTCGACA
A20	3172	AOD	Non-symptomatic	Inner bark	AW	AGACGCACTC
A21	5008	AOD	Non-symptomatic	Sapwood	AW	AGCACTGTAG
A22	1524	AOD	Non-symptomatic	Heartwood	AW	ATCAGACACG
A23 *	4870	AOD	Symptomatic	Outer bark	AW	ATATCGCGAG
A24 *	7765	AOD	Symptomatic	Inner bark	AW	CGTGTCTCTA
A25 *	10540	AOD	Symptomatic	Sapwood	AW	CTCGCGTGTC
A26 *	6306	AOD	Symptomatic	Heartwood	AW	TAGTATCAGC
A27 *	5994	AOD	Symptomatic	Gallery	AW	TCTCTATGCG
A28 *	2996	AOD	Non-symptomatic	Outer bark	AW	TGATACGTCT
A29 *	4971	AOD	Non-symptomatic	Inner bark	AW	TACTGAGCTA
A30 *	6072	AOD	Non-symptomatic	Sapwood	AW	ACGAGTGCGT
A31 *	2730	AOD	Non-symptomatic	Heartwood	AW	ACGCTCGACA

Table 1. *Cont.*

Sample	Sequences after Denoising	Symptom Status of Tree	Symptom Status of Tissue	Tissue	Site	Barcode Sequence
B2	12559	Healthy	Healthy	Inner bark	BW	ACGAGTGCGT
B3	13716	Healthy	Healthy	Sapwood	BW	ACGCTCGACA
B6 *	7248	AOD	Symptomatic	Inner bark	BW	AGACGCACTC
B7 *	7907	AOD	Symptomatic	Sapwood	BW	AGCACTGTAG
B9 *	10338	AOD	Symptomatic	Gallery	BW	ATCAGACACG
B11 *	19265	AOD	Non-symptomatic	Inner bark	BW	ATATCGCGAG
B12 *	9824	AOD	Non-symptomatic	Sapwood	BW	CGTGTCTCTA
SB2	12491	Healthy	Healthy	Inner bark	SB	ACGAGTGCGT
SB3	7845	Healthy	Healthy	Sapwood	SB	ACGCTCGACA
SB6 *	6759	AOD	Symptomatic	Inner bark	SB	AGACGCACTC
SB7 *	9311	AOD	Symptomatic	Sapwood	SB	AGCACTGTAG
SB11 *	7031	AOD	Non-symptomatic	Inner bark	SB	ATCAGACACG
SB12 *	5127	AOD	Non-symptomatic	Sapwood	SB	ATATCGCGAG
SB9 *	12471	AOD	Symptomatic	Gallery	SB	CGTGTCTCTA

* Tree displayed advanced stages of the syndrome; GMW: Great Monks Wood; SB: Stratfield Brake; BW: Bisham Wood; AW: Attingham Wood; RW: Runs Wood.

2.2. Bacterial Communities Associated with Oak Tissue

Genomic DNA was extracted from different tissue samples using a CTAB DNA extraction protocol as follows: From each sample, between 600 and 700 mg of material were scraped into a weigh boat using disposable scalpels. After weighing, the material was transferred into a clean bore mill canister (Kleco, Visalia, CA, USA) containing a 2.5 cm ball bearing. 7.5 mL of prepared CTAB buffer (100 mM Tris-HCl, pH 8.0, 2% CTAB (Cetyltrimethylammoniumbromide), 20 mM EDTA, 1.4 M NaCl) including freshly added 1.0% sodium sulphite, 2.0% PVP-40 and 1% antifoam agent (A5757, Sigma, Gillingham, Dorset, UK) were then added to each canister which was subsequently sealed with a lid and o-ring. Canisters were loaded onto a ball mill (Kleco) and the samples were ground for 2 min. After grinding, 1 mL of extract was transferred with a pipette into a 2 mL tube for incubation at 65 °C for 10–15 min. 1 mL chloroform:isoamyl alcohol (24:1) were added and mixed by inverting followed by centrifugation at 11,000× *g* for 10 min. The aqueous (top) layer was transferred to a new tube. This process was repeated once. An equal volume of ice cold isopropanol and 0.5 volumes 5 M NaCl were added to the crude DNA extract, which was incubated at −20 °C for 30 min. After centrifugation at 13,000× *g* for 10 min the supernatant was discarded and the pellet was washed by addition of 400 µL of 70% ethanol followed by centrifugation at 13,000× *g* for 4 min. The ethanol was discarded and the pellet dried for 5 min. The pellet was resuspended in 100 µL molecular grade water (Severn Biotech, Kidderminster, UK). Since DNA extracts from specific tissues contained large amounts of phenolic substances, DNA extracts were further purified by gel electrophoresis. For this, 20 to 25 µL of DNA extract were run on a 0.8% agarose gel and the band containing high molecular weight DNA was excised. It was then purified using the UltraClean® GelSpin® DNA Extraction Kit (MoBio, Carlsbad, CA, USA) following the manufacturer's instructions followed by storage at −20 °C.

Bacterial community structure was assessed based on the V3–V5 region of the 16S rRNA gene [39]. PCR primers flanking this region were adapted to 454 amplicon sequencing. For the forward primer a 25-mer Lib-L specific sequence adapter (underlined) was followed by a 454 amplicon sequencing specific 4-mer amplification key (italic) which was accompanied by a 10-mer barcode sequence to aid multiplexing (NNNN) and the template specific primer sequence (bold), specifically primer 341f (5′-CCATCTCATCCCTGCGTGTCTCCGAC*TCAG*NNNN**CCTACGGGNGGCWGCAG**-3′). For the reverse primer a 25-mer Lib-L specific sequence adapter (underlined) was followed by the target primer (bold) specifically 805r (5′-CCTATCCCCTGTGTGCCTTGGCAGTCTCAG**GACTACHVGGGTATCTAATCC**-3′). An overview of the barcode sequences can be found in Table 1. Amplification reactions of 20 µL were carried out using the Phusion High-Fidelity DNA Polymerase (New England Biolabs, Hitchin, UK) containing 4 µL of HF buffer, 0.3 µM of forward and reverse primers respectively, 0.3 mM of dNTPs, 0.4 U Phusion DNA polymerase and 1 µL of template DNA. The final reaction volume was made up with nuclease-free water (Severn Biotech). Amplification was carried out on a C1000 thermal cycler (BioRad, Hercules, CA, USA) starting with an initial single denaturing step at 98 °C for 2 min, followed by 25 cycles of denaturation at 98 °C for 10 s, annealing at 55 °C for 30 s and extension at 72 °C for 30 s, followed by a final extension at 72 °C for 10 min. PCR products containing unique barcodes were pooled aiming at equimolar concentrations. Gel purification was used to remove small DNA fragments from pooled amplicons prior to emulsion PCR, which was carried out according to Roche's instructions. Sequencing of all amplicons was completed using the GS FLX+ System (Roche, Burgess Hill, UK).

2.3. Data Analysis

Bioinformatics analysis was carried out using QIIME v1.90 [40] based on denoised data processed via FlowClus [41]. A minimum read length of 100 bp and a maximum read length of 500 bp were used. Quality filtering was applied removing reads with a Phred quality score (Q) less than 30 on average and those with less than Q25 across a 50 bp sliding window. A 1 bp mismatch in the primers and barcode sequences was allowed. Reads obtained per sample were highly variable ranging from 633 to 19,265 with an average of 5748 sequences. The QIIME protocol "de novo OTU

(Operational Taxonomic Unit) picking" [42] was used for clustering of the sequences followed by taxonomy assignment using the greengenes database (reference version gg_13_8_otus, [43]). In detail, OTUs were picked using uclust [44] utilizing the first seed as representative sequence. Pynast was subsequently utilized to align sequences [45] followed by taxonomy assignment via uclust [44]. After filtering of the alignment via pynast applying default values, a phylogenetic tree was constructed by fasttree [46]. ChimeraSlayer [47] was applied for detection of chimeric sequences. No chimeric sequences were found. The procedure was carried out on the 4 June 2015. Removal of OTUs assigned to chloroplasts, chlorophyta, mitochondria, archaea and sequences unassigned at kingdom level were removed from the dataset as described previously [6]. We observed a high variation in sequence number obtained for different samples as described previously [48]. To allow comparison of disparate libraries, normalization of sequence number is achieved by random selection of sequences referred to as rarefaction [49–55]. The effect of this process on beta diversity has been demonstrated [56–58]. However, other studies could not find an effect [59] or showed the importance of rarefaction to reduce bias in pyrosequencing datasets [49]. Therefore, libraries were rarefied to the same sequencing depth (1000 sequences). This resulted in loss of data for samples A5, A10, A22, A26, A31, R1, R2, R3, R4, R5, R6, R7, R8, R9, and R10. Singletons detected in the rarefied dataset were kept [59–62]. This approach was chosen since rare taxa can play an important role in the environment [63–66], whilst their role in health or disease is unclear [67]. Thus, it is important to study such taxa instead of dismissing them [68].

Differences in alpha (within sample) diversity were assessed by comparing the number of OTUs, chao1 richness estimator [69] and phylogenetic diversity (PD, [70]) obtained for each sample based on the rarefied dataset. Relative abundances of OTUs clustered at 97% sequences similarity were used to assess differences between bacterial communities. Multivariate analysis of square root transformed community data was performed using the subroutines nonmetric multidimensional scaling (nMDS) and analysis of similarities (ANOSIM, [71]) based on Bray–Curtis similarities of the PRIMER software package version 7 (Primer-E Ltd., Lutton, UK). Clustering was applied using complete linkage mode. Phylogenetic analysis was performed by MEGA 6 [72,73] using alignment by ClustalW followed by the Maximum Likelihood method based on the Jukes-Cantor model.

2.4. Nucleotide Sequence Accession Numbers

The 16S rRNA gene sequences derived from pyrosequencing have been deposited in the European Nucleotide Archive under study accession number PRJEB12457 (sample accession numbers ERS1037713—ERS1037800).

3. Results and Discussion

We studied the composition of bacterial communities associated with oak tissues from trees with and without disease symptoms at five sites in England. In total, 15 trees were sampled, five without disease symptoms (called healthy) and ten with disease symptoms. In addition, panels without symptoms were tested from diseased trees (non-symptomatic samples) (Table 1). In total 88 tissue samples were processed. We first present results of the overall community structure and relative composition at the family and genus level and then consider results according to tree health status.

3.1. Total Oak Microbiome

In total, we detected 8354 different OTUs at 97% sequence similarity level representing different bacterial taxa. Of these 5764 OTUs were singletons. The phyla Proteobacteria (Alpha-, Beta-, Delta- and Gamma-Proteobacteria), Firmicutes, Bacteroidetes, Actinobacteria, Tenericutes, Chloroflexi, Planctomycetes, Synergistetes, Verrucomicrobia and Gemmatimonadetes were most prominent, but also members of the phyla Deinococcus-Thermus, Acidobacteria, Armatimonadetes, Caldiserica, Chlamydiae, Chlorobi, Cyanobacteria, Deferribacteres, Fibrobacteres, Lentisphaerae, Nitrospirae,

Spirochaetes, Thermotogae and relatives of the candidate phyla BRC1, FBP, LD1, NKB19, OD1, OP8, OP9, SAR406, SR1, TM7, WPS-2, WS4, WS6 and WWE1 were found.

Overall, the most abundant 20 taxa belonged to the following families or orders: Pseudomonadaceae (OTU 1542, 18% and OTU 15320, 1.1%), Enterobacteriaceae (OTU 5035, 8.7%; OTU 22973, 1.7%; OTU 8983, 0.9%), Halomonadaceae (OTU 21506; 5.6%), Shewanellaceae (OTU 12625, 2.1%), Acholeplasmataceae (OTUs 26072 and 15330, 2% each), Bacillales (OTU 29261, 1.5%), Anaerolinaceae (OTU 24991, 1.1%), Micrococcaceae (OTU 14189, 1%), Bacteroidales (OTU 5809, 0.8% and OTU 26954, 0.7%), Lachnospiraceae (OTU 10815, 0.8%), Syntrophomonadaceae (OTU 18748, 0.8%), Tissierellia (OTU 28647, 0.7%), Planctomycetaceae (OTU 15334, 0.7%) and uncultured Firmicutes (OTU 14625, 1.7% and OTU 21451, 0.9%) as illustrated in Figure 1. The most abundant members of the community at each site varied. At AW, BW and SB these were members of the Proteobacteria (OTU 1542 and OTU 21506 or OTU 5035), whereas Firmicutes and Actinobacteria (OTUs 29261 and 14189) or Proteobacteria and Firmicutes (OTUs 5035 and 14625) dominated at GMW and RW, respectively.

It needs to be noted that species level identification is hindered in this dataset due to the limited taxonomic resolution of the 16S rRNA gene for specific groups like the Enterobacteriaceae, for which other markers may be more suitable [74,75]. It is thus thought that classical pathogen detection could be complemented with metabarcoding approaches if relevant targets like the gyrase B gene [74] are chosen. However, the lack of sequence information for a wide range of taxa currently hinders the broad use of such markers in microbial ecology. Since this is the first molecular report on the composition of the oak microbiome at a range of sites we selected a broad taxonomic marker to gain an initial overview. Furthermore, sequencing errors introduced by pyrosequencing were eliminated by using a stringent quality control approach that included the latest algorithm for denoising of the raw data via FlowClus [41].

Species diversity (number of OTUs and Shannon diversity) and estimated richness (chao1) varied greatly with highest values found in samples from GMW followed by RW. Lowest diversity and PD (phylogenetic diversity) were observed in samples from BW (Table 2). Community structure varied most between samples from different locations as illustrated in Figure 2. GMW showed the strongest difference from other locations followed by samples from RW. However, some similarities in communities were observed for samples from BW, SB and AW. The overall separation was confirmed by ANOSIM (Global $R = 0.816$, $p = 0.001$). Pairwise comparisons indicated significant differences among sites apart from BW and SB, which were very similar in community composition. Both sites had considerably lower OTU numbers and the phylogenetic diversity was lower than in the other three sites (Table 2). The number of taxa detected at all sites was generally comparable to the phyllosphere microbiome consisting of several hundred or less taxa [6,13–16].

By comparison, alpha diversity values were far greater at the sites GMW and RW for which the chao1 richness estimator indicated a taxon diversity with thousands of different taxa but still not reaching the richness observed in the rhizosphere, where tens of thousands of taxa have been commonly recorded [10–12,76]. For these samples, we did not achieve the coverage required to describe the full diversity of these samples. Nevertheless, we are convinced that the present analysis describes differences for the most common taxa found in our samples as suggested previously [77].

The different oak tissue types (sapwood, heartwood, *etc.*) did not display a consistent separation across all sites as indicated by ANOSIM (Global $R = -0.041$, $p = 0.894$). This implicates, that spatial structuring at the level of tissues did not override site specific differences. However, when the gallery associated bacteria from all sites were compared with all of those associated with heartwood, significant differences were found in pairwise comparison ($R = 0.151$, $p = 0.037$).

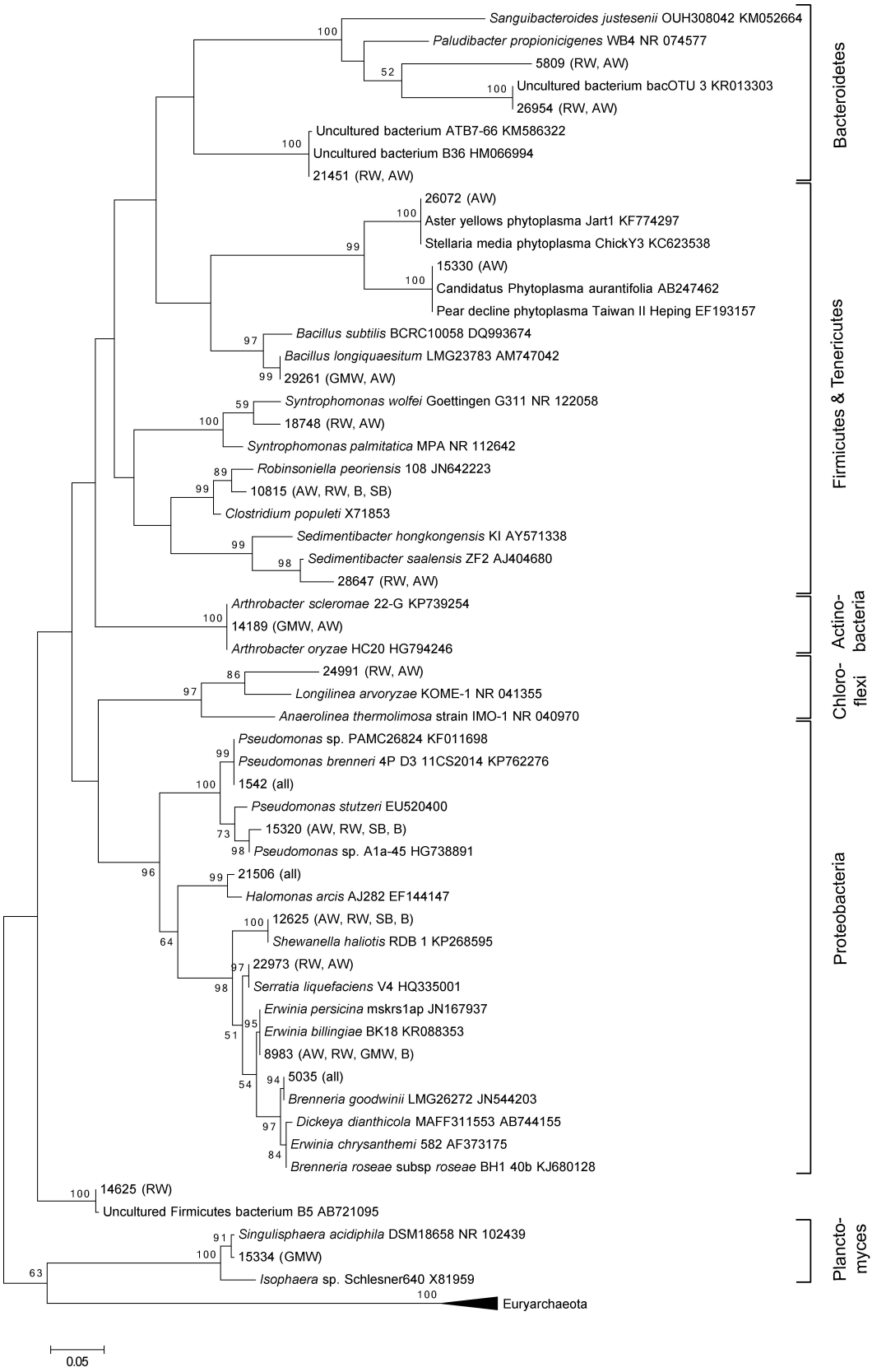

Figure 1. Phylogenetic tree of the 20 most abundant oak associated bacteria, irrespective of health status of the tissue. Bootstrap values above 50% are displayed. Sites where the OTUs were detected are indicated in brackets (Attingham Wood (AW), Runs Wood (RW), Great Monks Wood (GMW), Stratfield Brake (SB), Bisham (BW)).

Table 2. Overview of alpha diversity of bacterial communities.

Sample ID	No OTUs	Richness Chao1	Shannon Diversity H′(log2)	PD †
GMW2	516	2499	7.86	52.57
GMW3	495	2783	7.63	51.32
GMW6	472	2170	7.47	50.73
GMW7	505	2007	7.72	51.15
GMW9	471	1609	7.65	49.65
GMW11	482	2030	7.64	49.96
GMW12	459	2084	7.39	47.74
GMW6 *	454	1598	7.55	48.69
GMW7 *	469	2052	7.55	51.53
GMW9 *	512	3307	7.81	52.43
GMW11 *	480	2020	7.66	49.31
GMW12 *	465	2087	7.52	51.05
R11	550	2607	8.03	68.33
R12	543	2828	8.00	63.92
R13	552	2695	8.02	65.34
R14	604	2522	8.46	73.48
R15	508	2053	7.87	65.01
R16	227	855	5.34	32.01
R17	279	774	6.12	41.90
R18	121	447	2.16	21.76
R19	388	1173	7.07	56.14
R20	400	1392	7.35	53.29
R21	388	1016	7.21	53.43
R22	347	1053	7.05	50.83
R23 *	277	781	5.85	44.63
R24 *	128	351	2.37	26.69
R25 *	122	345	2.46	25.39
R26 *	349	995	7.00	50.94
R27 *	99	233	1.75	19.48
R28 *	404	1057	7.73	57.80
R29 *	348	903	7.25	54.40
R30 *	337	964	6.89	48.95
R31 *	329	872	6.84	49.47
A1	23	32	2.01	6.05
A2	95	169	3.68	16.46
A3	54	101	3.03	11.63
A4	204	341	5.98	37.49
A6	103	180	3.79	16.79
A7	59	107	2.96	11.77
A8	180	317	5.28	28.59
A9	114	194	3.83	19.84
A11	28	46	2.22	7.97
A12	132	229	4.00	25.72
A13	188	349	5.12	25.59
A14	185	313	6.23	25.04
A15	46	60	3.27	10.11
A16	144	306	4.68	22.85
A17	126	344	3.71	20.06
A18	151	494	4.60	27.46
A19	107	222	4.16	16.44
A20	32	56	2.40	7.43
A21	104	282	3.61	18.39
A23 *	106	194	4.85	16.80
A24 *	167	303	5.69	21.11
A25 *	87	152	4.17	16.60
A27 *	158	417	4.77	28.99
A28 *	166	384	4.53	31.77
A29 *	63	119	2.86	15.65
A30 *	167	317	5.76	32.26
B2	27	53	0.94	6.89
B3	28	85	0.90	7.38
B6 *	58	94	2.69	10.66
B7 *	30	240	1.05	6.79
B9 *	57	135	2.65	11.00
B11 *	35	64	1.33	8.41
B12 *	15	20	0.74	4.13
SB2	24	29	0.75	6.46
SB3	29	53	0.96	7.59
SB6 *	158	424	5.06	20.85
SB7 *	182	426	5.38	23.60
SB11 *	18	63	0.55	3.99
SB12 *	28	52	0.88	8.79
SB9 *	69	102	3.92	13.02

* Tree displayed advanced stages of the syndrome; † Phylogenetic Diversity.

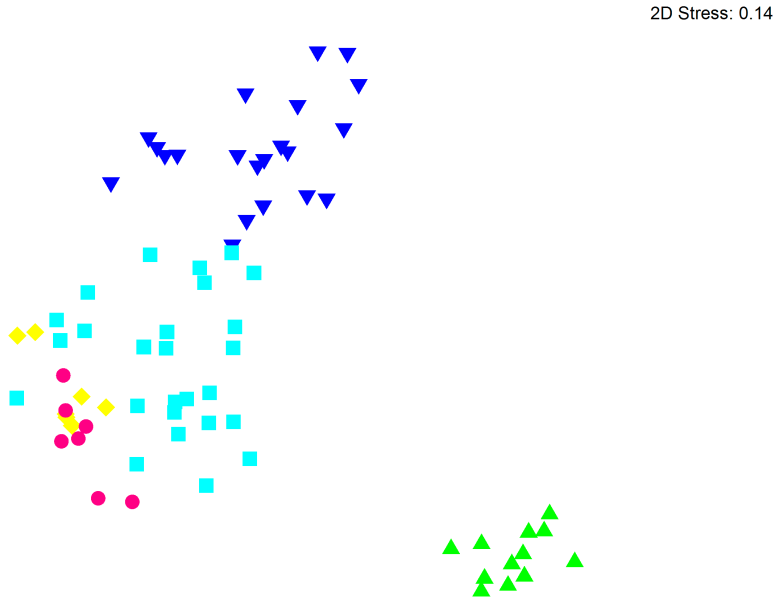

Figure 2. NMDS plot based on Bray–Curtis similarities of relative bacterial abundances after square root transformation. Displayed are the communities from the following sites: Attingham Wood (■), Runs Wood (▼), Great Monks Wood (▲), Stratfield Brake (●), Bisham Wood (●).

To identify taxa representing the oak microbiome we used the core microbiome algorithm available via QIIME. We identified that a phylotype belonging to the genus Pseudomonas, Gammaproteobacteria (OTU 1542) was found in 95% of samples regardless of health status or tissue type. This phylotype was accompanied by a member of the genus Halomonas (Gammaproteobacteria) in up to 80% of samples (OTU 21506).

Similar to studies of other plant organs, Proteobacteria dominated the communities associated with oak tissue and included the presence of Bacteroidetes and Firmicutes [6,13,15,19,78–81]. Interestingly, Juncker *et al.* [6] identified a member of the Gammaproteobacteria (Enterobacteriaceae) as dominant in stamina and styles whereas a member of the Pseudomonadaceae was identified as dominant in the oak microbiome. Our finding is in line with findings from Ottesen *et al.* [7], who also detected dominance by members of the Pseudomonadaceae and Micrococcineae on tomato fruit samples.

Geographical distance appeared to shape the oak microbiome implicating strong spatial structuring and adaptation to the local environment which was also shown previously on Tamarix trees [14]. On a smaller scale, spatial structuring was not apparent for the various oak tissues examined within the trees, although we assumed that they would differ considerably in the microniches provided to bacteria. However, we detected a significant difference between galleries and heartwood supporting the hypothesis for the two most discerned tissues.

3.2. Bacterial Community Structure in Relation to the Tree's Health Status

The link between the health status of a tree or specific tissue and its microbiome was tested using ANOSIM. There was no significant difference between the total microbial communities from healthy and diseased trees (Global $R = 0.106$, $p = 0.090$). However, we could detect a relationship between the oaks' microbiomes and the health status of the tissue (Global $R = 0.091$, $p = 0.001$), which was strengthened when the trees' health status was also taken into account (Global $R = 0.151$, $p = 0.001$). For comparison of samples with varying sequence depth we applied random sampling of sequences, which can cause overestimation of β-diversity [57]. Thus, we limited our analyses to major shifts and differences detected between samples.

Healthy Trees: When identifying the subset of OTUs indicative of a healthy oak microbiome, the phylotypes 1542 and 21506 as well as a member of the genus Shewanella (Gammaproteobacteria, OTU 12625) were identified for 80% of healthy samples. Two members of the Proteobacteria, namely OTUs 15035 and 8364, (Achromobacter (Betaproteobacteria) and Stenotrophomonas (Gammaproteobacteria) respectively) were detected in seven of nine healthy samples.

Diseased trees: Advanced symptom tissues only: The oak microbiome of trees displaying advanced stages of the AOD syndrome was indicated by the phylotype 5035, a member of the family Enterobacteriaceae, Gammaproteobacteria, in 80% of samples. Phylogenetic analysis indicated a close relationship to *Brenneria goodwinii* previously isolated from AOD tissue [33] supporting its important role in the syndrome. Although it was also detected in healthy tissue, its levels were increased drastically, where symptoms were observed. Additionally, other enteric taxa detected in this study showed a close relationship to plant pathogenic bacteria like Erwinia [82] implying a role in the acute oak decline syndrome. Additionally, members of the Tenericutes [83,84] were detected at one site, but these occurred also in healthy tissue contradicting a unique contribution to the symptoms seen in symptomatic tissue.

Since OTU 1542 was also present in 80% of samples from symptomatic tissue, it is assumed that this phylotype is generally associated with oak tissue regardless of health status. Pseudomonas species were described as plant endophytes before ([85] and references therein) with *P. stutzeri* being described as denitrifying organism [86] with antifungal activity [87] suggesting a beneficial role in its interaction with the plant. In contrast, Firmicutes like relatives of *Robinsoniella peoriensis* are involved in the degradation of cellobiose [88], a metabolite in cellulose degradation indicating a saprophytic lifestyle.

Due to the high site-specific variability observed, we analyzed the datasets per site with regards to the health status of the tissues (Figure 3). We observed a strong link between microbiomes and tissue health supported by ANOSIM at the sites AW (Global $R = 0.299$, $p = 0.001$), RW (Global $R = 0.395$, $p = 0.001$) and SB (Global $R = 1$, $p = 0.029$). In contrast, associated bacteria at the sites BW and GMW were not significantly correlated with the health status of the tissue. Hence, metabarcoding was unable to detect a strong signature for an AOD associated microbiome.

In summary, the overall health status of the trees had only a very small effect on the general oak microbiome, which indicates that there was no common shift towards a disease indicating community across the sites studied. This implies, that the whole bacterial community does not shift drastically towards a disease indicator microbiome independent of site. Instead, rather small global effects are observed by AOD in symptomatic tissue, presumably masked by location specific signatures. This is supported by the finding, that specific sites did display distinct shifts in oak associated communities for symptomatic tissues, especially in advanced stages when signatures from other sites were removed. This finding implies that the observed shifts are dependent on geographical conditions highlighting that spatial structuring occurs regardless of the studied AOD syndrome being apparent. In future studies, tree age or specific composition of the plant's metabolites and phenolic compounds could be included to characterize the tissues analyzed. Furthermore, the height of the samples' origin will be of interest as highlighted previously [7]. Such information would describe the microniche, the bacteria reside in, allowing a correlation between such characteristics and community structure. The latter requires the development of taxonomic targets that are suitable for high throughput sequencing and complement 16S rRNA gene sequencing by providing higher taxonomic resolution for families like the Enterobactericeae. In addition, the influence of other microorganisms present should be studied including fungi, microeukaryotes and viruses. For the identification of novel putative disease causing organisms site independent characteristics like metabolites would also be beneficial, to allow the identification of bacteria solely changing in relation to the health status of the trees studied. Furthermore, an assessment of tree associated microbiomes covering the present variety of tree species in a given location should be taken into account. Although we could not detect a distinct shift in the microbiome due to AOD, we could confirm the recurring presence of previously isolated Enterobacteriaceae, namely *Brenneria goodwinii* in symptomatic tissue.

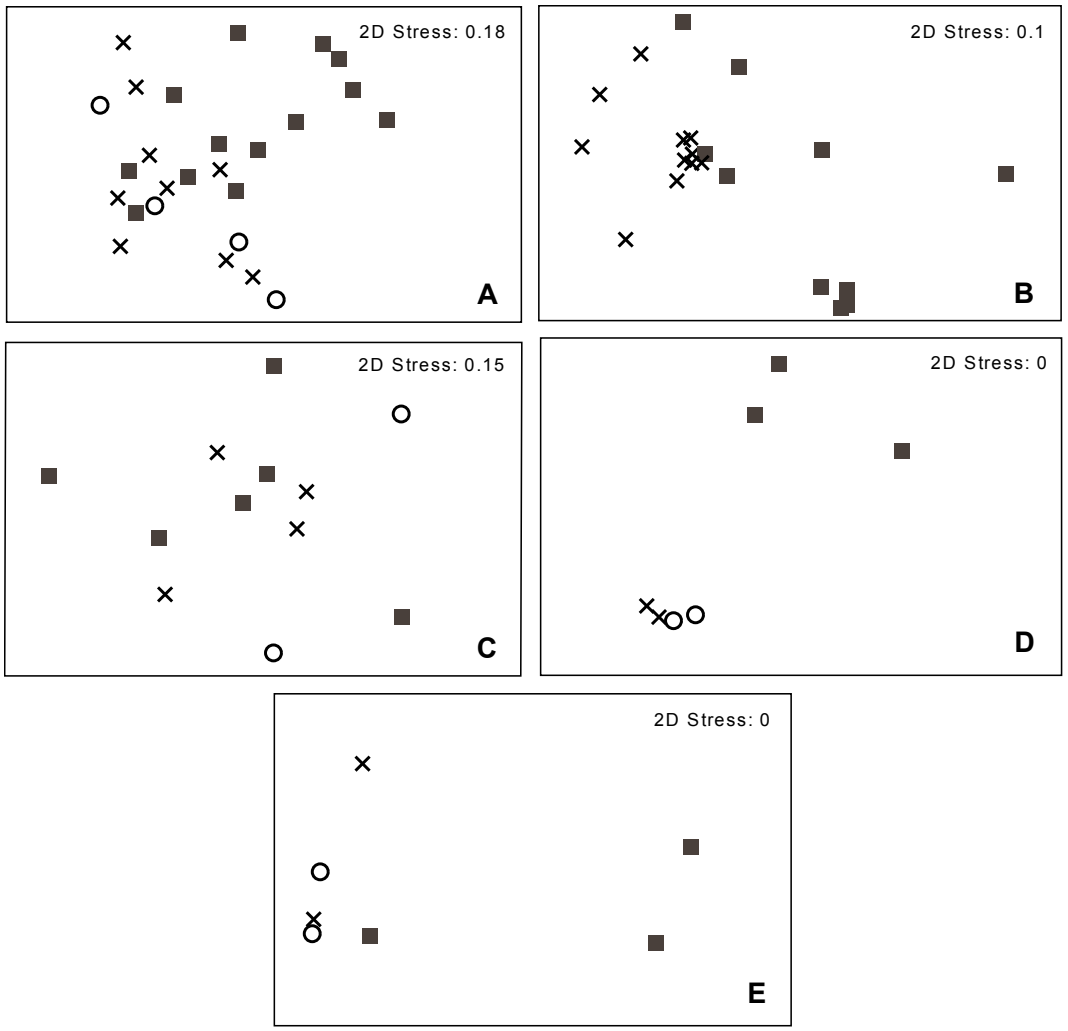

Figure 3. NMDS plot based on Bray–Curtis similarities of relative bacterial abundances after square root transformation in relation to the health status of the tissue sampled including all samples. Tissue health status was categorized as non-symptomatic tissues from trees with AOD (✖), symptomatic tissues from trees with AOD (■) and healthy tissue (○). Displayed are the communities from the following sites: Attingham Wood (**A**); Runs Wood (**B**); Great Monks Wood (**C**); Stratfield Brake (**D**); Bisham Wood (**E**).

4. Conclusions

We demonstrated that strong site-specific signatures exist for oak associated bacteria studied in various tissues. The number of phylotypes ranged from several hundreds to below hundred. Apart from this variability we could identify two taxa mainly associated with tissue from healthy trees belonging to the Gammaproteobacteria. Due to the high variability between sites we could not detect a distinct shift towards an acute oak decline syndrome associated microbiome. However, one phylotype (OTU 5035) belonging to the Enterobacteriaceae was consistently found at elevated levels in symptomatic tissues at all sites suggesting a role of this bacterium in the AOD syndrome. Furthermore, members of the Firmicutes were abundant at most sites highlighting their importance in oak-prokaryote interactions. This study offers a so far unknown description of oak associated microbiomes using a metabarcoding approach on a wide range of sites.

Acknowledgments: This work was supported by funding from the UK Department of Environment Food and Rural Affairs (Defra), project TH0108 and the Forestry Commission. We are grateful to Hez Hird for initial material processing and thank Richard Thwaites for fruitful discussions.

Author Contributions: Melanie Sapp coordinated the molecular microbiome analyses at Fera, performed QIIME and statistical analyses and prepared the main components of this manuscript. Erin Lewis carried out the preparations of 16S rDNA libraries followed by pyrosequencing. She helped with manuscript writing which also holds true for Stephen Moss, who also performed quality control and denoising of the pyrosequencing data. Ben Barrett extracted DNA from the studied oak samples applying his own improved procedure and contributed to the manuscript. Susan Kirk catalogued all oak tissues analyzed in this study. John Elphinstone helped conceptualize the study, provided guidance with detection of plant pathogens as well as plant associated microbiomes and helped writing the manuscript. Sandra Denman conceptualized the study, developed the sampling design, carried out the field sampling, provided guidance on the acute oak decline syndrome and helped with writing the manuscript.

Conflicts of Interest: The authors declare no conflict of interest.

References

1. Denman, S.; Brown, N.; Kirk, S.; Jeger, M.; Webber, J. A description of the symptoms of Acute Oak Decline in Britain and a comparative review on causes of similar disorders on oak in Europe. *Forestry* **2014**, *87*, 535–551. [CrossRef]
2. Brown, N.; Jeger, M.; Kirk, S.; Xu, X.; Denman, S. Spatial and temporal patterns in symptom expression within eight woodlands affected by Acute Oak Decline. *For. Ecol. Manag.* **2016**, *360*, 97–109. [CrossRef]
3. Denman, S.; Webber, J.F. Oak declines—New definitions and new episodes in Britain. *Q. J. For.* **2009**, *103*, 285–290.
4. Andrews, J.H.; Harris, R.F. The Ecology and Biogeography of Microorganisms on Plant Surfaces. *Annu. Rev. Phytopathol.* **2000**, *38*, 145–180. [CrossRef] [PubMed]
5. Grice, E.A.; Kong, H.H.; Conlan, S.; Deming, C.B.; Davis, J.; Young, A.C.; Program, N.C.S.; Bouffard, G.G.; Blakesley, R.W.; Murray, P.R.; *et al.* Topographical and temporal diversity of the human skin microbiome. *Science* **2009**, *324*, 1190–1192. [CrossRef] [PubMed]
6. Junker, R.R.; Keller, A. Microhabitat heterogeneity across leaves and flower organs promotes bacterial diversity. *FEMS Microbiol. Ecol.* **2015**, *91*. [CrossRef] [PubMed]
7. Ottesen, A.R.; González Peña, A.; White, J.R.; Pettengill, J.B.; Li, C.; Allard, S.; Rideout, S.; Allard, M.; Hill, T.; Evans, P.; *et al.* Baseline survey of the anatomical microbial ecology of an important food plant: *Solanum lycopersicum* (tomato). *BMC Microbiol.* **2013**, *13*, 114. [CrossRef] [PubMed]
8. Berg, G.; Grube, M.; Schloter, M.; Smalla, K. Unraveling the plant microbiome: Looking back and future perspectives. *Front. Microbiol.* **2014**, *5*, 1–7.
9. Bulgarelli, D.; Schlaeppi, K.; Spaepen, S.; van Themaat, E.V.L.; Schulze-Lefert, P. Structure and functions of the bacterial microbiota of plants. *Annu. Rev. Plant Biol.* **2013**, *64*, 807–838. [CrossRef] [PubMed]
10. Berendsen, R.L.; Pieterse, C.M.J.; Bakker, P.A. The rhizosphere microbiome and plant health. *Trends Plant Sci.* **2012**, *17*, 478–486. [CrossRef] [PubMed]
11. Roesch, L.F.W.; Fulthorpe, R.R.; Riva, A.; Casella, G.; Km, A.; Kent, A.D.; Daroub, S.H.; Camargo, F.A.O.; Farmerie, W.G.; Triplett, E.W. Pyrosequencing enumerates and contracts soil microbial diversity. *ISME J.* **2007**, *1*, 283–290. [PubMed]
12. Weinert, N.; Piceno, Y.; Ding, G.-C.; Meincke, R.; Heuer, H.; Berg, G.; Schloter, M.; Andersen, G.; Smalla, K. PhyloChip hybridization uncovered an enormous bacterial diversity in the rhizosphere of different potato cultivars: Many common and few cultivar-dependent taxa. *FEMS Microbiol. Ecol.* **2011**, *75*, 497–506. [CrossRef] [PubMed]
13. Leff, J.W.; Del Tredici, P.; Friedman, W.E.; Fierer, N. Spatial structuring of bacterial communities within individual *Ginkgo biloba* trees. *Environ. Microbiol.* **2015**, *17*, 2352–2361. [CrossRef] [PubMed]
14. Finkel, O.M.; Burch, A.Y.; Lindow, S.E.; Post, A.F.; Belkin, S. Geographical location determines the population structure in phyllosphere microbial communities of a salt-excreting desert tree. *Appl. Environ. Microbiol.* **2011**, *77*, 7647–7655. [CrossRef] [PubMed]
15. Lambais, M.R.; Crowley, D.E.; Cury, J.C.; Büll, R.C.; Rodrigues, R.R. Bacterial diversity in tree canopies of the atlantic forest. *Science* **2006**, *312*, 1917. [CrossRef] [PubMed]
16. Kembel, S.W.; O'Connor, T.K.; Arnold, H.K.; Hubbell, S.P.; Wright, S.J.; Green, J.L. Relationships between phyllosphere bacterial communities and plant functional traits in a neotropical forest. *Proc. Natl. Acad. Sci. USA* **2014**, *111*, 13715–13720. [CrossRef] [PubMed]

17. Lindow, S.E.; Brandl, M.T. MINIREVIEW: Microbiology of the phyllosphere. *Appl. Environ. Microbiol.* **2003**, *69*, 1875–1883. [CrossRef] [PubMed]
18. Bodenhausen, N.; Bortfeld-Miller, M.; Ackermann, M.; Vorholt, J.A. A synthetic community approach reveals plant genotypes affecting the Phyllosphere Microbiota. *PLoS Genet.* **2014**, *10*, e1004283. [CrossRef] [PubMed]
19. Whipps, J.M.; Hand, P.; Pink, D.; Bending, G.D. Phyllosphere microbiology with special reference to diversity and plant genotype. *J. Appl. Microbiol.* **2008**, *105*, 1744–1755. [CrossRef] [PubMed]
20. Barbaroux, C.; Bréda, N. Contrasting distribution and seasonal dynamics of carbohydrate reserves in stem wood of adult ring-porous sessile oak and diffuse-porous beech trees. *Tree Physiol.* **2002**, *22*, 1201–1210. [CrossRef] [PubMed]
21. Zhang, B.; Cai, J.; Duan, C.-Q.; Reeves, M.; He, F. A Review of polyphenolics in oak woods. *Int. J. Mol. Sci.* **2015**, *16*, 6978–7014. [CrossRef] [PubMed]
22. Doussot, F.; Pardon, P.; Dedier, J.; De Jeso, B. Individual, species and geographic origin influence on cooperage oak extractible content (*Quercus robur* L. and *Quercus petraea* Liebl.). *Analusis* **2000**, *28*, 960–965. [CrossRef]
23. De Simón, B.F.; Hernández, T.; Cadahía, E.; Dueñas, M.; Estrella, I. Phenolic compounds in a Spanish red wine aged in barrels made of Spanish, French and American oak wood. *Eur. Food Res. Technol.* **2003**, *216*, 150–156.
24. Prida, A.; Puech, J.L. Influence of geographical origin and botanical species on the content of extractives in American, French, and East European oak woods. *J. Agric. Food Chem.* **2006**, *54*, 8115–8126. [CrossRef] [PubMed]
25. Biosca, E.G.; González, R.; López-López, M.J.; Soria, S.; Montón, C.; Pérez-Laorga, E.; López, M.M. Isolation and characterization of *Brenneria quercina*, causal agent for bark canker and drippy nut of *Quercus* spp. in Spain. *Phytopathology* **2003**, *93*, 485–492. [CrossRef] [PubMed]
26. González, R.; López-López, M.J.; Biosca, E.G.; López, F.; Santiago, R.; López, M.M. First report of bacterial deep bark canker of walnut caused by *Brenneria* (*Erwinia*) *rubrifaciens* in Europe. *Plant Dis.* **2002**, *86*, 696. [CrossRef]
27. Maes, M.; Huvenne, H.; Messens, E. *Brenneria salicis*, the bacterium causing watermark disease in willow, resides as an endophyte in wood. *Environ. Microbiol.* **2009**, *11*, 1453–1462. [CrossRef] [PubMed]
28. Schmidt, O.; Dujesiefken, D.; Stobbe, H.; Moreth, U.; Kehr, R.; Schröder, T. *Pseudomonas syringae* pv. *aesculi* associated with horse chestnut bleeding canker in Germany. *For. Pathol.* **2008**, *38*, 124–128.
29. Webber, J.F.; Parkinson, N.M.; Rose, J.; Stanford, H.; Cook, R.T.A.; Elphinstone, J.G. Isolation and identification of *Pseudomonas syringae* pv. *aesculi* causing bleeding canker of horse chestnut in the UK. *Plant Pathol.* **2008**, *57*, 368. [CrossRef]
30. Lebeis, S.L.; Rott, M.; Dangl, J.L.; Schulze-Lefert, P. Culturing a plant microbiome community at the cross-Rhodes. *New Phytol.* **2012**, *196*, 341–344. [CrossRef] [PubMed]
31. Brady, C.; Denman, S.; Kirk, S.; Venter, S.; Rodríguez-Palenzuela, P.; Coutinho, T. Description of *Gibbsiella quercinecans* gen. nov., sp. nov., associated with Acute Oak Decline. *Syst. Appl. Microbiol.* **2010**, *33*, 444–450. [CrossRef] [PubMed]
32. Brady, C.L.; Cleenwerck, I.; Denman, S.; Venter, S.N.; Rodríguez-Palenzuela, P.; Coutinho, T.A.; De Vos, P. Proposal to reclassify *Brenneria quercina* (Hildebrand and Schroth 1967) Hauben *et al.* 1999 into a new genus, *Lonsdalea* gen. nov., as *Lonsdalea quercina* comb. nov., descriptions of *Lonsdalea quercina* subsp. *quercina* comb. nov., *Lonsdalea quercina* subsp. ib. *Int. J. Syst. Evol. Microbiol.* **2012**, *62*, 1592–1602. [CrossRef] [PubMed]
33. Denman, S.; Brady, C.; Kirk, S.; Cleenwerck, I.; Venter, S.; Coutinho, T.; De Vos, P. *Brenneria goodwinii* sp. nov., associated with acute oak decline in the UK. *Int. J. Syst. Evol. Microbiol.* **2012**, *62*, 2451–2456. [CrossRef] [PubMed]
34. Brady, C.; Hunter, G.; Kirk, S.; Arnold, D.; Denman, S. *Gibbsiella greigii* sp. nov., a novel species associated with oak decline in the USA. *Syst. Appl. Microbiol.* **2014**, *37*, 417–422. [CrossRef] [PubMed]
35. Brady, C.; Hunter, G.; Kirk, S.; Arnold, D.; Denman, S. *Rahnella victoriana* sp. nov., *Rahnella bruchi* sp. nov., *Rahnella woolbedingensis* sp. nov., classification of Rahnella genomospecies 2 and 3 as *Rahnella variigena* sp. nov. and *Rahnella inusitata* sp. nov., respectively and emended description of the genus *Rahnella*. *Syst. Appl. Microbiol.* **2014**, *37*, 545–552. [PubMed]
36. Brady, C.; Hunter, G.; Kirk, S.; Arnold, D.; Denman, S. Description of *Brenneria roseae* sp. nov. and two subspecies, *Brenneria roseae* subspecies *roseae* ssp. nov and *Brenneria roseae* subspecies *americana* ssp. nov. isolated from symptomatic oak. *Syst. Appl. Microbiol.* **2014**, *37*, 396–401. [CrossRef] [PubMed]

37. Peplies, J.; Kottmann, R.; Ludwig, W.; Glöckner, F.O. A standard operating procedure for phylogenetic inference (SOPPI) using (rRNA) marker genes. *Syst. Appl. Microbiol.* **2008**, *31*, 251–257. [CrossRef] [PubMed]
38. Tremblay, J.; Singh, K.; Fern, A.; Kirton, E.S.; He, S.; Woyke, T.; Lee, J.; Chen, F.; Dangl, J.L.; Tringe, S.G. Primer and platform effects on 16S rRNA tag sequencing. *Front. Microbiol.* **2015**, *6*, 771. [CrossRef] [PubMed]
39. Klindworth, A.; Pruesse, E.; Schweer, T.; Peplies, J.; Quast, C.; Horn, M.; Glockner, F.O. Evaluation of general 16S ribosomal RNA gene PCR primers for classical and next-generation sequencing-based diversity studies. *Nucleic Acids Res.* **2013**, *41*, e1. [CrossRef] [PubMed]
40. Caporaso, J.G.; Kuczynski, J.; Stombaugh, J.; Bittinger, K.; Bushman, F.D.; Costello, E.K.; Fierer, N.; Peña, A.G.; Goodrich, J.K.; Gordon, J.I.; *et al.* QIIME allows analysis of high-throughput community sequencing data. *Nat. Methods* **2010**, *7*, 335–336. [CrossRef] [PubMed]
41. Gaspar, J.M.; Thomas, W.K. FlowClus: Efficiently filtering and denoising pyrosequenced amplicons. *BMC Bioinform.* **2015**, *16*, 105. [CrossRef] [PubMed]
42. Rideout, J.R.; He, Y.; Navas-molina, J.A.; Walters, W.A.; Ursell, L.K.; Gibbons, S.M.; Chase, J.; Mcdonald, D.; Gonzalez, A.; Robbins-pianka, A.; *et al.* Subsampled open-reference clustering creates consistent, comprehensive OTU definitions and scales to billions of sequences. *PeerJ* **2014**, *2*, e545. [CrossRef] [PubMed]
43. DeSantis, T.Z.; Hugenholtz, P.; Larsen, N.; Rojas, M.; Brodie, E.L.; Keller, K.; Huber, T.; Dalevi, D.; Hu, P.; Andersen, G.L. Greengenes, a chimera-checked 16S rRNA gene database and workbench compatible with ARB. *Appl. Environ. Microbiol.* **2006**, *72*, 5069–5072. [CrossRef] [PubMed]
44. Edgar, R.C. Search and clustering orders of magnitude faster than BLAST. *Bioinformatics* **2010**, *26*, 2460–2461. [CrossRef] [PubMed]
45. Caporaso, J.G.; Bittinger, K.; Bushman, F.D.; DeSantis, T.Z.; Andersen, G.L.; Knight, R. PyNAST: A flexible tool for aligning sequences to a template alignment. *Bioinformatics* **2010**, *26*, 266–267. [CrossRef] [PubMed]
46. Price, M.N.; Dehal, P.S.; Arkin, A.P. FastTree 2—Approximately maximum-likelihood trees for large alignments. *PLoS ONE* **2010**, *5*, e9490. [CrossRef] [PubMed]
47. Haas, B.J.; Gevers, D.; Earl, A.M.; Feldgarden, M.; Ward, D.V.; Giannoukos, G.; Ciulla, D.; Tabbaa, D.; Highlander, S.K.; Sodergren, E.; *et al.* Chimeric 16S rRNA sequence formation and detection in Sanger and 454-pyrosequenced PCR amplicons. *Genome Res.* **2011**, *21*, 494–504. [CrossRef] [PubMed]
48. Harris, J.K.; Sahl, J.W.; Castoe, T.A.; Wagner, B.D.; Pollock, D.D.; Spear, J.R. Comparison of Normalization Methods for construction of large, multiplex amplicon pools for next-generation sequencing. *Appl. Environ. Microbiol.* **2010**, *76*, 3863–3868. [CrossRef] [PubMed]
49. Gihring, T.M.; Green, S.J.; Schadt, C.W. Massively parallel rRNA gene sequencing exacerbates the potential for biased community diversity comparisons due to variable library sizes. *Environ. Microbiol.* **2012**, *14*, 285–290. [CrossRef] [PubMed]
50. Flores, G.E.; Bates, S.T.; Caporaso, J.G.; Lauber, C.L.; Leff, J.W.; Knight, R.; Fierer, N. Diversity, distribution and sources of bacteria in residential kitchens. *Environ. Microbiol.* **2013**, *15*, 588–596. [CrossRef] [PubMed]
51. Krych, L.; Hansen, C.H.F.; Hansen, A.K.; van den Berg, F.W.J.; Nielsen, D.S. Quantitatively different, yet qualitatively alike: A meta-analysis of the mouse core gut microbiome with a view towards the human gut microbiome. *PLoS ONE* **2013**, *8*, e62578. [CrossRef] [PubMed]
52. Leff, J.W.; Fierer, N. Bacterial communities associated with the surfaces of fresh fruits and vegetables. *PLoS ONE* **2013**, *8*, e59310. [CrossRef] [PubMed]
53. Prober, S.M.; Leff, J.W.; Bates, S.T.; Borer, E.T.; Firn, J.; Harpole, W.S.; Lind, E.M.; Seabloom, E.W.; Adler, P.B.; Bakker, J.D.; *et al.* Plant diversity predicts beta but not alpha diversity of soil microbes across grasslands worldwide. *Ecol. Lett.* **2015**, *18*, 85–95. [CrossRef] [PubMed]
54. Zhang, X.; Qu, Y.; Ma, Q.; Zhang, Z.; Li, D.; Wang, J.; Shen, W.; Shen, E.; Zhou, J. Illumina MiSeq sequencing reveals diverse microbial communities of activated sludge systems stimulated by different aromatics for indigo biosynthesis from indole. *PLoS ONE* **2015**, *10*, e0125732. [CrossRef] [PubMed]
55. Smith, C.C.R.; Snowberg, L.K.; Gregory Caporaso, J.; Knight, R.; Bolnick, D.I. Dietary input of microbes and host genetic variation shape among-population differences in stickleback gut microbiota. *ISME J.* **2015**, *9*, 2515–2526. [CrossRef] [PubMed]
56. McMurdie, P.J.; Holmes, S. Waste Not, Want Not: Why Rarefying Microbiome Data Is Inadmissible. *PLoS Comput. Biol.* **2014**, *10*, e1003531. [CrossRef] [PubMed]

57. Zhou, J.; Jiang, Y.-H.; Deng, Y.; Shi, Z.; Zhou, B.Y.; Xue, K.; Wu, L.; He, Z.; Yang, Y. Random sampling process leads to overestimation of β-diversity of microbial communities. *mBio* **2013**, *4*, e00324-13. [CrossRef] [PubMed]
58. De Cárcer, D.A.; Denman, S.E.; McSweeney, C.; Morrison, M. Evaluation of subsampling-based normalization strategies for tagged high-throughput sequencing data sets from gut microbiomes. *Appl. Environ. Microbiol.* **2011**, *77*, 8795–8798. [CrossRef] [PubMed]
59. Lallias, D.; Hiddink, J.G.; Fonseca, V.G.; Gaspar, J.M.; Sung, W.; Neill, S.P.; Barnes, N.; Ferrero, T.; Hall, N.; Lambshead, P.J.D.; *et al.* Environmental metabarcoding reveals heterogeneous drivers of microbial eukaryote diversity in contrasting estuarine ecosystems. *ISME J.* **2015**, *9*, 1208–1221. [CrossRef] [PubMed]
60. Bendtsen, K.M.B.; Krych, L.; Sørensen, D.B.; Pang, W.; Nielsen, D.S.; Josefsen, K.; Hansen, L.H.; Sørensen, S.J.; Hansen, A.K. Gut microbiota composition is correlated to grid floor induced stress and behavior in the BALB/c mouse. *PLoS ONE* **2012**, *7*, e46231.
61. Ren, G.; Zhang, H.; Lin, X.; Zhu, J.; Jia, Z. Response of leaf endophytic bacterial community to elevated CO_2 at different growth stages of rice plant. *Front. Microbiol.* **2015**, *6*, 855. [CrossRef] [PubMed]
62. Touceda-González, M.; Brader, G.; Antonielli, L.; Ravindran, V.B.; Waldner, G.; Friesl-Hanl, W.; Corretto, E.; Campisano, A.; Pancher, M.; Sessitsch, A. Combined amendment of immobilizers and the plant growth-promoting strain *Burkholderia phytofirmans* PsJN favours plant growth and reduces heavy metal uptake. *Soil Biol. Biochem.* **2015**, *91*, 140–150. [CrossRef]
63. Elshahed, M.S.; Youssef, N.H.; Spain, A.M.; Sheik, C.; Najar, F.Z.; Sukharnikov, L.O.; Roe, B.A.; Davis, J.P.; Schloss, P.D.; Bailey, V.L.; *et al.* Novelty and uniqueness patterns of rare members of the soil biosphere. *Appl. Environ. Microbiol.* **2008**, *74*, 5422–5428. [CrossRef] [PubMed]
64. Galand, P.E.; Casamayor, E.O.; Kirchman, D.L.; Lovejoy, C. Ecology of the rare microbial biosphere of the Arctic Ocean. *Proc. Natl. Acad. Sci. USA* **2009**, *106*, 22427–22432. [CrossRef] [PubMed]
65. Sogin, M.L.; Morrison, H.G.; Huber, J.A.; Welch, D.M.; Huse, S.M.; Neal, P.R.; Arrieta, J.M.; Herndl, G.J. Microbial diversity in the deep sea and the underexplored "rare biosphere". *Proc. Natl. Acad. Sci. USA* **2006**, *103*, 12115–12120. [CrossRef] [PubMed]
66. Van Dorst, J.; Bissett, A.; Palmer, A.S.; Brown, M.; Snape, I.; Stark, J.S.; Raymond, B.; McKinlay, J.; Ji, M.; Winsley, T.; *et al.* Community fingerprinting in a sequencing world. *FEMS Microbiol. Ecol.* **2014**, *89*, 316–330. [CrossRef] [PubMed]
67. Caporaso, J.G.; Lauber, C.L.; Walters, W.A.; Berg-Lyons, D.; Lozupone, C.A.; Turnbaugh, P.J.; Fierer, N.; Knight, R. Global patterns of 16S rRNA diversity at a depth of millions of sequences per sample. *Proc. Natl. Acad. Sci. USA* **2011**, *108*, 4516–4522. [CrossRef] [PubMed]
68. Zinger, L.; Gobet, A.; Pommier, T. Two decades of describing the unseen majority of aquatic microbial diversity. *Mol. Ecol.* **2012**, *21*, 1878–1896. [CrossRef] [PubMed]
69. Goodman, L.A. On the estimation of the number of classes in a population. *Ann. Math. Stat.* **1949**, *20*, 572–579. [CrossRef]
70. Faith, D.P. Conservation evaluation and phylogenetic diversity. *Biol. Conserv.* **1992**, *61*, 1–10. [CrossRef]
71. Sapp, M.; Schwaderer, A.S.; Wiltshire, K.H.; Hoppe, H.-G.; Gerdts, G.; Wichels, A. Species-specific bacterial communities in the phycosphere of microalgae? *Microb. Ecol.* **2007**, *53*, 683–699. [CrossRef] [PubMed]
72. Jukes, T.H.; Cantor, C.R. Evolution of protein molecules. *Mamm. Protein Metab.* **1969**, *3*, 21–132.
73. Tamura, K.; Stecher, G.; Peterson, D.; Filipski, A.; Kumar, S. MEGA6: Molecular Evolutionary genetics analysis version 6.0. *Mol. Biol. Evol.* **2013**, *30*, 2725–2729. [CrossRef] [PubMed]
74. Delmas, J.; Breysse, F.; Devulder, G.; Flandrois, J.-P.; Chomarat, M. Rapid identification of Enterobacteriaceae by sequencing DNA gyrase subunit B encoding gene. *Diagn. Microbiol. Infect. Dis.* **2006**, *55*, 263–268. [CrossRef] [PubMed]
75. Wang, L.-T.; Lee, F.-L.; Tai, C.-J.; Kasai, H. Comparison of gyrB gene sequences, 16S rRNA gene sequences and DNA-DNA hybridization in the *Bacillus subtilis* group. *Int. J. Syst. Evol. Microbiol.* **2007**, *57*, 1846–1850. [CrossRef] [PubMed]
76. Mendes, R.; Kruijt, M.; de Bruijn, I.; Dekkers, E.; van der Voort, M.; Schneider, J.H.M.; Piceno, Y.M.; DeSantis, T.Z.; Andersen, G.L.; Bakker, P.A.; *et al.* Deciphering the rhizosphere microbiome for disease-suppressive bacteria. *Science* **2011**, *332*, 1097–1100. [CrossRef] [PubMed]

77. Lundin, D.; Severin, I.; Logue, J.B.; Östman, Ö.; Andersson, A.F.; Lindström, E.S. Which sequencing depth is sufficient to describe patterns in bacterial α-and β-diversity? *Environ. Microbiol. Rep.* **2012**, *4*, 367–372. [CrossRef] [PubMed]
78. Idris, R.; Trifonova, R.; Puschenreiter, M.; Wenzel, W.W.; Sessitsch, A. Bacterial communities associated with flowering plants of the Ni hyperaccumulator Thlaspi goesingense. *Appl. Environ. Microbiol.* **2004**, *70*, 2667–2677. [CrossRef] [PubMed]
79. Stapleton, A.E.; Simmons, S.J. Plant control of phyllosphere diversity: Genotype interactions with ultraviolet-B radiation. In *Microbial Ecology of Aerial Plant Surfaces*; Bailey, M., Lilley, A., Timms-Wilson, T., Spencer-Phillips, P., Eds.; CAB International: Wallingford, UK, 2006; pp. 223–238.
80. Rasche, F.; Marco-Noales, E.; Velvis, H.; van Overbeek, L.S.; López, M.M.; van Elsas, J.D.; Sessitsch, A. Structural characteristics and plant-beneficial effects of bacteria colonizing the shoots of field grown conventional and genetically modified T4-lysozyme producing potatoes. *Plant Soil* **2006**, *289*, 123–140. [CrossRef]
81. Rasche, F.; Trondl, R.; Naglreiter, C.; Reichenauer, T.G.; Sessitsch, A. Chilling and cultivar type affect the diversity of bacterial endophytes colonizing sweet pepper (*Capsicum anuum* L.). *Can. J. Microbiol.* **2006**, *52*, 1036–1045. [CrossRef] [PubMed]
82. Starr, M.P.; Chatterjee, A.K. The genus Erwinia: Enterobacteria pathogenic to plants and animals. *Annu. Rev. Microbiol.* **1972**, *26*, 389–426. [CrossRef] [PubMed]
83. Gasparich, G.E. Spiroplasmas and phytoplasmas: Microbes associated with plant hosts. *Biologicals* **2010**, *38*, 193–203. [CrossRef] [PubMed]
84. Lee, I.-M.; Gundersen-Rindal, D.E.; Bertaccini, A. Phytoplasma: Ecology and genomic diversity. *Phytopathology* **1998**, *88*, 1359–1366. [CrossRef] [PubMed]
85. Hardoim, P.R.; van Overbeek, L.S.; van Elsas, J.D. Properties of bacterial endophytes and their proposed role in plant growth. *Trends Microbiol.* **2008**, *16*, 463–471. [CrossRef] [PubMed]
86. Lalucat, J.; Bennasar, A.; Bosch, R.; García-Valdés, E.; Palleroni, N.J. Biology of *Pseudomonas stutzeri*. *Microbiol. Mol. Biol. Rev.* **2006**, *70*, 510–547. [CrossRef] [PubMed]
87. Lim, H.S.; Kim, Y.S.; Kim, S.D. *Pseudomonas stutzeri* YPL-1 genetic transformation and antifungal mechanism against *Fusarium solani*, an agent of plant root rot. *Appl. Environ. Microbiol.* **1991**, *57*, 510–516. [PubMed]
88. Cotta, M.A.; Whitehead, T.R.; Falsen, E.; Moore, E.; Lawson, P.A. *Robinsoniella peoriensis* gen. nov., sp. nov., isolated from a swine-manure storage pit and a human clinical source. *Int. J. Syst. Evol. Microbiol.* **2009**, *59*, 150–155. [CrossRef] [PubMed]